© 2018. Published by The Company of Biologists Ltd | Development (2018) 145, dev157784. doi:10.1242/dev.157784

RESEARCH ARTICLE

Floral homeotic proteins modulate the genetic program for leaf development to suppress trichome formation in flowers

Diarmuid S. Ó'Maoiléidigh[1,2,*,‡], Darragh Stewart[1,*], Beibei Zheng[1], George Coupland[2] and Frank Wellmer[1]

ABSTRACT

As originally proposed by Goethe in 1790, floral organs are derived from leaf-like structures. The conversion of leaves into different types of floral organ is mediated by floral homeotic proteins, which, as described by the ABCE model of flower development, act in a combinatorial manner. However, how these transcription factors bring about this transformation process is not well understood. We have previously shown that floral homeotic proteins are involved in suppressing the formation of branched trichomes, a hallmark of leaf development, on reproductive floral organs of *Arabidopsis*. Here, we present evidence that the activities of the C function gene *AGAMOUS* (*AG*) and the related *SHATTERPROOF1/2* genes are superimposed onto the regulatory network that controls the distribution of trichome formation in an age-dependent manner. We show that *AG* regulates cytokinin responses and genetically interacts with the organ polarity gene *KANADI1* to suppress trichome initiation on gynoecia. Thus, our results show that parts of the genetic program for leaf development remain active during flower formation but have been partially rewired through the activities of the floral homeotic proteins.

KEY WORDS: ABCE model, Floral homeotic proteins, Flower development, Trichome development, Cytokinin

INTRODUCTION

A unifying theory in plant biology is that modifications of a central growth plan underlie the development of the various tissues and organs (Coen and Carpenter, 1993). This idea is well illustrated by the 'metamorphosis' of leaves to floral organs (von Goethe, 1790), which gained support on a molecular level when mutants of a number of floral homeotic genes were combined. These higher-order mutants produced leaf-like structures in place of floral organs (Bowman et al., 1991; Ditta et al., 2004), whereas ectopic expression of the corresponding transcription factors transformed leaves into floral organs (Honma and Goto, 2001; Pelaz et al., 2001). The floral homeotic proteins contain MADS DNA-binding domains and form multimeric complexes to control flower formation in a partially overlapping manner (Ó'Maoiléidigh et al., 2014). Briefly, in *Arabidopsis*, APETALA1 (AP1) controls sepal and petal formation, APETALA3 (AP3) and PISTILLATA (PI) control petal and stamen formation, whereas AGAMOUS (AG) controls stamen and carpel formation. The SEPALLATA1-4 (SEP1-4) proteins mediate the specification of all floral organ types and are thought to be essential for the formation of quaternary MADS protein complexes (Immink et al., 2009; Theissen, 2001). The activities of these transcription factors are summarized in the ABCE and floral quartet models (Krizek and Fletcher, 2005; Ó'Maoiléidigh et al., 2014; Theissen, 2001), which represent major steps forward in our understanding of how floral organs derived from leaves. However, the genetic and molecular mechanisms underlying this conversion process remain poorly understood.

To address this knowledge gap, genomic approaches have been successfully applied to identify target genes of the floral organ identity factors (Ó'Maoiléidigh et al., 2014). From these studies, we know that, for example, AG promotes the expression of several known regulators of stamen and carpel formation, such as *CRABS CLAW* (*CRC*), *SPOROCYTELESS* (*SPL*) and *SUPERMAN* (*SUP*), indicating that it controls the expression of a battery of apparently flower-specific factors to generate floral organs (Gomez-Mena et al., 2005; Ito et al., 2004; Ó'Maoiléidigh et al., 2013). These analyses also offered the first glimpses of the interactions between the floral organ identity factors and the underlying leaf development program. AG was found to suppress the expression of genes with peak expression in leaves, many of which are involved in photosynthesis (Ó'Maoiléidigh et al., 2013). Moreover, AG was shown to suppress the formation of branched trichomes (hairs), a hallmark of leaf development (Bowman et al., 1991, 1989; Ditta et al., 2004), on carpel valves by controlling key regulatory genes (Ó'Maoiléidigh et al., 2013).

In *Arabidopsis*, single-celled trichomes form on the epidermal surfaces of leaves and inflorescence stems, although their distribution on these organs is age dependent (Chien and Sussex, 1996; Telfer et al., 1997). By contrast, floral organs, with the exception of sepals of early-arising flowers, are devoid of trichomes (Smyth et al., 1990). The gradual decline in trichome density with aging is regulated by the transcription factor-encoding *SQUAMOSA PROMOTER BINDING-LIKE* (SPL) genes (Yu et al., 2010). Activity of several SPL genes is post-transcriptionally regulated by *microRNA156* (*miR156*), expression of which decreases in an age-dependent manner (Wang et al., 2009; Wu and Poethig, 2006). The subsequent increase in *SPL* activity contributes to a gradual reduction in trichome initiation on successive cauline leaves, stem internodes and sepals (Shikata et al., 2009; Yu et al., 2010), as well as to trichome formation being shifted from the adaxial (upper) to abaxial (lower) side of leaves (Chien and Sussex, 1996; Telfer et al., 1997). Phytohormones also influence trichome distribution and density during development (Maes et al., 2008). In particular, *GLABROUS INFLORESCENCE STEMS* (*GIS*), *GIS2* and *ZINC FINGER PROTEIN 8* (*ZFP8*), which encode C2H2 transcription factors that are induced by cytokinin and gibberellin, control trichome distribution on leaves, stems and sepals by promoting *GLABRA1* (*GL1*) expression (Gan et al., 2007). These regulators appear to function independently of the SPLs (Yu et al., 2010).

[1]Smurfit Institute of Genetics, Trinity College Dublin, Ireland. [2]Department of Plant Developmental Biology, Max Planck Institute for Plant Breeding Research, D-50829 Cologne, Germany.
*These authors contributed equally to this work

‡Author for correspondence (omaoil@mpipz.mpg.de)

D.S.Ó'M., 0000-0002-3043-3750; G.C., 0000-0001-6988-4172; F.W., 0000-0002-2095-0981

Received 28 July 2017; Accepted 2 January 2018

Development (2018) 145, dev157784. doi:10.1242/dev.157784

Whereas the reproductive floral organs and petals of *Arabidopsis* are glabrous, many angiosperm species form abaxial trichomes on gynoecia to protect developing fruits and seed pods from herbivory. These include members of the Brassicaceae (the family to which *Arabidopsis* belongs), such as *Sinapis alba* (white mustard) (Lamb, 1980), and members of the genus *Erysimum* (wallflower), which, remarkably, form trichomes not only abaxially, but also on the inside of carpel valves (Czarna et al., 2016). Thus, there is considerable diversity in trichome initiation patterns even among closely related flowering plants.

To improve our understanding of the control of trichome formation in flowers, we combined data from transcriptomics and genome-wide localization studies with detailed genetic analysis. Here, we present evidence that the suppression of trichomes on reproductive organs by floral homeotic proteins is largely superimposed onto the regulatory network that controls the distribution of trichome formation throughout plant development in an age- and organ polarity-dependent manner. Furthermore, we show that AG acts in this process by suppressing cytokinin signaling in the gynoecium. These results contribute to the establishment of a mechanistic framework to understand how floral organs form from leaf-like structures.

RESULTS

AGAMOUS and *SHATTERPROOF1/2* act together to suppress trichome initiation on gynoecia

We previously showed that a conditional knockdown of the C function regulator *AG*, which is mediated by the expression of an artificial microRNA (amiRNA) against *AG* from an ethanol-inducible promoter system (denoted AG-amiRNA^{AlcR}), led to the formation of trichomes on carpel valves (Ó'Maoiléidigh et al., 2013). Given that this phenotype was weak, with only few trichomes forming per gynoecium, we considered whether additional regulators contribute to the suppression of floral trichomes. Candidates for genes that might act redundantly with *AG* in this process are the *SHATTERPROOF1* (*SHP1*) and *SHP2* genes, which are closely related to *AG*, and together control aspects of fruit development and ovule identity (Liljegren et al., 2000; Pinyopich et al., 2003). Furthermore, it has been shown that ectopic expression of *SHP2* can partly substitute for AG activity (Pinyopich et al., 2003). To test whether *AG* and the *SHP* genes act redundantly in the control of trichome initiation in the gynoecium, we introgressed the AG-amiRNA^{AlcR} transgene into a *shp1 shp2* double mutant, in which gynoecia are hairless (Liljegren et al., 2000). After induction of AG-amiRNA expression, AG-amiRNA^{AlcR} *shp1 shp2* gynoecia (Fig. 1C,D) bore significantly (P<0.001) more trichomes on their abaxial surfaces than those of equally treated AG-amiRNA^{AlcR} plants (Fig. 1A,B) (13.5±0.5 for AG-amiRNA^{AlcR} *shp1 shp2* versus 8.0±0.3 for AG-amiRNA^{AlcR}; see Table 1 for a summary of trichome counts presented in this study and for the results of statistical tests; all values quoted represent the mean and s.e.m. of trichome counts; Table S1 contains additional details on the statistical tests performed). Conversely, conditional overexpression of a functional SHP2-GFP fusion protein from a dexamethasone-inducible promoter system (denoted SHP2-GFP$^{GR\text{-}LhG4}$; Fig. S1) largely suppressed trichome initiation on carpel valves after *AG* perturbation (2.2±0.2 for AG-amiRNA^{AlcR} SHP2-GFP$^{GR\text{-}LhG4}$ plants treated with both ethanol and dexamethasone versus 8.8±0.5 for plants of the same genotype treated with ethanol alone; P<0.001) (Fig. 1E,F; Table 1). Taken together, these results indicate that a conserved function of these floral MADS domain proteins is the suppression of trichome initiation on gynoecia.

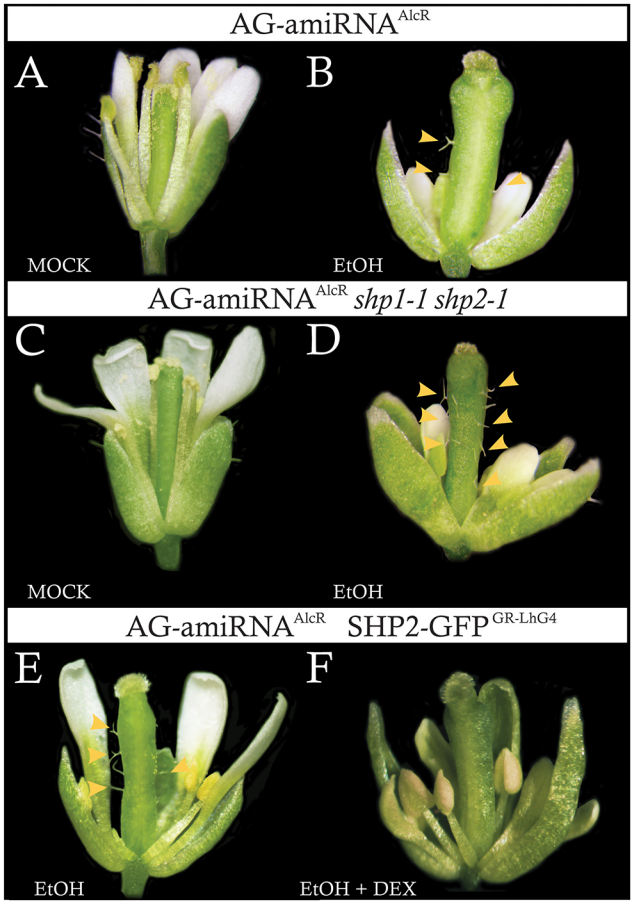

Fig. 1. SHP1/2 are involved in the suppression of trichome formation on gynoecia. The AG-amiRNA^{AlcR} line is based on the ethanol-responsive behavior of the AlcR transcription factor, which can induce AG-amiRNA expression. Trichomes form on the abaxial side of carpel valves after ethanol treatment in all plants, although the phenotype is stage dependent. (A,B) Flowers from AG-amiRNA^{AlcR} plants after (A) mock treatment and (B) ethanol vapor treatment. (C,D) Flowers from AG-amiRNA^{AlcR} *shp1 shp2* plants after (C) mock treatment and (D) ethanol (EtOH) vapor treatment. (E,F) Flowers from AG-amiRNA^{AlcR} SHP2-GFP$^{GR\text{-}LhG4}$ plants after (E) ethanol vapor treatment and (F) simultaneous ethanol vapor and dexamethasone (DEX) treatments. Arrowheads indicate simple or two branched trichomes. See Table 1 for details.

Interplay between trichome regulators and floral homeotic genes

The formation of trichomes on gynoecia is, as expected, fully dependent on the activity of the trichome initiation complex, which was first identified and characterized in leaves (Oppenheimer et al., 1991; Payne et al., 2000; Walker et al., 1999; Zhao et al., 2008). When we introgressed the AG-amiRNA^{AlcR} transgene into loss-of-function mutants for components of this complex [*GL1*, *TRANSPARENT TESTA GLABRA1* (*TTG1*), *GLABRA3* (*GL3*) and *ENHANCER OF GLABARA3* (*EGL3*)] or for *GLABRA2* (*GL2*), which acts directly downstream of the trichome initiation complex and mediates trichome development (Szymanski et al., 1998; Zhao et al., 2008), and knocked down *AG* activity in the resulting lines, trichome initiation on carpel valves was completely suppressed (Fig. S2; Table 1). Given that we had previously found that AG binds to the regulatory region of *GL1* and suppresses its expression (Ó'Maoiléidigh et al., 2013), it appears likely that the C function regulator inhibits trichome formation in part by limiting the activity of the trichome initiation complex. However, the results from an

Development (2018) 145, dev157784. doi:10.1242/dev.157784

Table 1. Summary of trichome counts presented in this study

Genotype	Treatment	Mean	s.e.m.	*n*	*P*
AG-amiRNA^{AlcR}	EtOH	8.0	0.3	204	–
	EtOH+MOCK	8.6	0.5	96	n.s.*
	EtOH+100 µM GA_3	12.6	0.6	112	<0.001‡
	EtOH+100 µM MeJA	13.9	0.6	129	<0.001‡
	EtOH+10 µM BAP	14.6	0.5	80	<0.001‡
	EtOH+50 µM BAP	18.8	1.0	75	<0.001‡
	EtOH+100 µM BAP	24.3	0.7	210	<0.001‡
AG-amiRNA^{AlcR} *shp1-1 shp2-1*	EtOH	13.5	0.5	78	<0.001*
AG-amiRNA^{AlcR} SHP2-GFP$^{GR-LhG4}$	EtOH	8.8	0.5	50	–
AG-amiRNA^{AlcR} SHP2-GFP$^{GR-LhG4}$	EtOH+10 µM DEX	2.2	0.2	86	<0.001*
AG-amiRNA^{AlcR} *cpc-1*	EtOH	10.8	0.5	66	<0.001‡
AG-amiRNA^{AlcR} *cpc-1*	EtOH+100 µM BAP	22.2	1.1	92	n.s.‡
AG-amiRNA^{AlcR} *try-29760*	EtOH	15.4	0.7	78	<0.001‡
AG-amiRNA^{AlcR} *try-29760*	EtOH+100 µM BAP	27.0	2.2	106	n.s.‡
AG-amiRNA^{AlcR} *try-29760 cpc-1*	EtOH	16.7	1.8	19	<0.001‡
AG-amiRNA^{AlcR} *try-29760 cpc-1*	EtOH+100 µM BAP	>35¶	–	25	<0.001‡
AG-amiRNA^{AlcR} miR156^{OE}	EtOH	21.2	0.6	103	<0.001‡
AG-amiRNA^{AlcR} MIM156 ^{OE}	EtOH	2.4	0.2	97	<0.001‡
AG-amiRNA^{AlcR} *spl9-4 spl15-1*	EtOH	18.1	0.6	50	<0.001‡
AG-amiRNA^{AlcR} *zfp8-1*	EtOH	1.5	0.2	97	<0.001‡
AG-amiRNA^{AlcR} *gis2-1*	EtOH	0.1	0.1	75	<0.001‡
AG-amiRNA^{AlcR} *kan1-11*	EtOH	26.6	0.8	50	<0.001*
AG-amiRNA^{AlcR} *kan1-11*	EtOH+100 µM BAP	32.2	0.8	50	<0.001*
AG-amiRNA^{AlcR} AP3-amiRNA$^{GR-LhG4}$ *try*-29760	EtOH+10 µM DEX	2.1§	0.3§	30	–
ag-10 try-29760	NT	16.0	0.9	30	–
ag-10 try-29760 cpc-1	NT	1.3§	0.2§	30	–
ag-10	100 µM BAP	23.7	1.1	30	–

DEX, dexamethasone; EtOH, ethanol vapor; MOCK, a mock solution; n.s., not significant; NT, no treatment.

For each analysis, the genotype of the plants used and the type of treatment is indicated, as well as the mean, s.e.m., sample size (*n*), and the results of statistical tests, if applicable. *P* values indicate the level of statistical significance relative to the appropriate control (see Table S1 for details). For all experiments shown, phenotypes were fully or almost fully (≥90%) penetrant. Numbers refer to trichomes on gynoecia unless indicated otherwise.

The following genotypes and/or treatments resulted in reproductive floral organs that were completely glabrous ($n \geq 50$): all lines containing the AG-amiRNA^{AlcR} transgene in which AG-amiRNA expression had not been induced through EtOH treatment, with the exception of AG-amiRNA^{AlcR} *try-29760 cpc-1* (see main text); *ag-10* (without treatment and after treatment with 100 µM MeJA or GA_3 or a mock solution), *try-29760*, *cpc-1*, *spl9-4 spl15-1*, *kan1-11*, *gis2-1*, *zfp8-1* mutants; ethanol-treated AG-amiRNA^{AlcR} plants containing SPL9pro:GFP-rSPL9, *gl1-20990*, *gl2-1*, *gl3-1 egl3-77439*, or *ttg1-1*; *cpc-1* after treatment with 100 µM BAP. Dexamethasone treatment of AG-amiRNA^{AlcR} plants had no discernible effect on trichome initiation patterns after AG perturbation.

*Two-tailed *t*-test.

‡One-way ANOVA followed by Holm–Šídák correction for multiple testing.

§Trichomes per anther.

¶Difficult to precisely quantify but larger than in any other experiment described in this study.

analysis of temporal gene expression during flower development (Ryan et al., 2015) implied an additional mechanism. We found that the expression of six of the seven R3-MYB transcription factor-coding genes, which function as negative regulators of trichome initiation (Wang et al., 2008), increases during early floral stages and remains high throughout flower development (Fig. 2A-C). Thus, these trichome repressor genes might contribute considerably to the suppression of trichome formation on floral organs. In agreement with this idea, we previously found that an *AG* knockdown in a mutant for one of these repressor genes, *TRIPTYCHON* (*TRY*), led to a strong increase in trichome numbers on gynoecia relative to AG-amiRNA^{AlcR} alone (Ó'Maoiléidigh et al., 2013). Likewise, gynoecia of double-mutant plants carrying the weak *ag-10* allele (Ji et al., 2011) and a strong mutant allele for *TRY* consistently carried trichomes on gynoecia (16.0±0.9), whereas the carpel valves of each single mutant were completely glabrous (Fig. S3A-D; Table 1).

We had previously found that the simultaneous perturbation of *AG* and the B function gene *PI* leads not only to the consistent formation of trichomes on gynoecia, but also occasionally to the initiation of one or two trichomes on the abaxial surface of anthers, a phenotype never observed after the separate knockdown of either of the two floral homeotic genes (Ó'Maoiléidigh et al., 2013). Thus, these regulators appear to act together in the suppression of trichome formation on stamens. We crossed the AG-amiRNA^{AlcR} with an AP3-amiRNA$^{GR-LhG4}$ line (Wuest et al., 2012), which allows the specific knockdown of the B function gene *AP3*, to confirm this observation and detected one or at most two trichomes on approximately 5% of anthers of plants treated with both ethanol and dexamethasone (Fig. S4A), but never on mock-treated control plants. To test whether the low penetrance and/or weakness of this phenotype was the result of trichome repressor gene activity in stamens, we introgressed a *try* mutant allele into the AG-amiRNA^{AlcR} AP3-amiRNA$^{GR-LhG4}$ background. A knockdown of *AG* and *AP3* activity in the resulting line led to a dramatic increase in the penetrance of the phenotype, with 2.1±0.3 trichomes forming on most (~90%) anthers (Fig. S4B,C; Table 1). Thus, *TRY* appears to be involved in the suppression of trichome formation on both male and female reproductive organs.

To understand the role of trichome repressor genes in floral organs better, we analyzed the function of *CAPRICE* (*CPC*), which acts in a partly redundant manner with *TRY* in leaves (Schellmann et al., 2002). Whereas gynoecia of *cpc* mutants prior to an *AG* knockdown were completely glabrous, after *AG* perturbation, they bore significantly ($P<0.001$) more trichomes than gynoecia of plants in which *AG* had been knocked down in a wild-type background (10.8±0.5 versus 8.0±0.3), but fewer than in *try* mutants

Development (2018) 145, dev157784. doi:10.1242/dev.157784

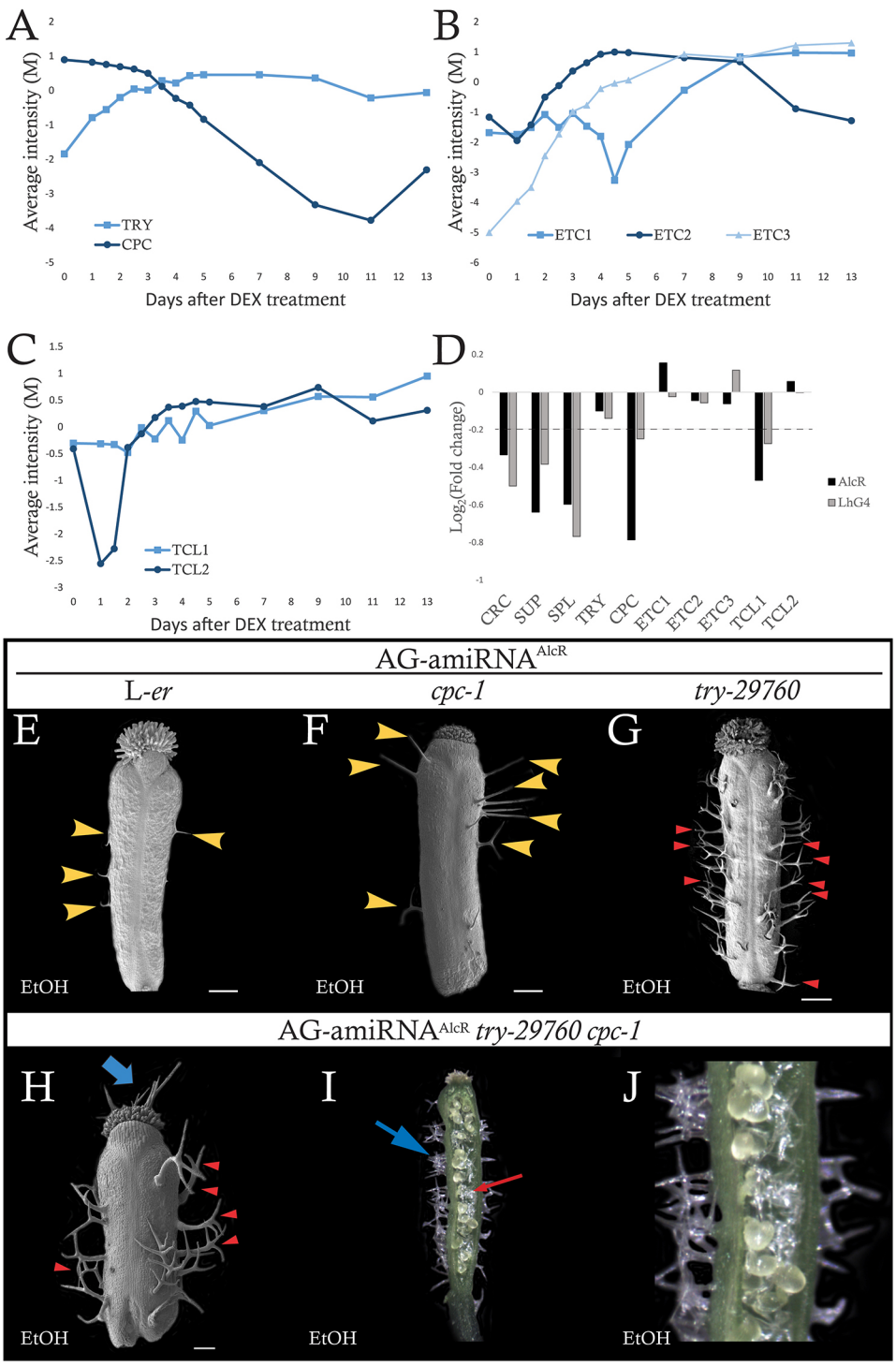

Fig. 2. Activity of repressors of trichome initiation during floral organ development. (A-C) Expression of trichome repressors (as indicated) from flower initiation (day 0) to maturation (day 13). Average signal intensities (M) from microarray experiments are shown (Ryan et al., 2015). (D) Expression of the same trichome repressors as in A-C after perturbation of *AG* activity via the AG-amiRNA driven by either an ethanol (AlcR) or dexamethasone-inducible (LhG4) promoter system relative to a mock-treated control (Ó'Maoiléidigh et al., 2015). Dashed line indicates the fold-change cut-off used to determine differentially expressed genes. *CRC*, *SUP* and *SPL* are known AG targets (Gomez-Mena et al., 2005; Ó'Maoiléidigh et al., 2013). (E-H) Scanning electron micrographs of gynoecia from ethanol (EtOH)-treated (E) AG-amiRNA^{AlcR}, (F) AG-amiRNA^{AlcR} *cpc*, (G) AG-amiRNA^{AlcR} *try* and (H) AG-amiRNA^{AlcR} *cpc try* plants. (I,J) A gynoecium from an ethanol-treated AG-amiRNA^{AlcR} *cpc try* plant with clusters of trichomes forming from the carpel valves (blue arrow). One carpel valve has been removed to display the formation of trichomes on the adaxial epidermis (red arrow). The blue arrow indicates the formation of trichome clusters on abaxial carpel valves. (J) A magnification of part of the image shown in I. Yellow and red arrowheads indicate simple or two-branched trichomes and three-branched trichomes, respectively. Scale bars: 200 µm. See Table 1 for details.

(15.4±0.7) (Fig. 2E-G; Table 1). We then generated AG-amiRNA^{AlcR} *try cpc* plants to test whether *TRY* and *CPC* also act redundantly in floral organs. Prior to *AG* perturbation, approximately 80% of AG-amiRNA^{AlcR} *try cpc* gynoecia were completely glabrous, whereas the remaining 20% formed one or two trichomes at their distal tip (Fig. S4D). By contrast, after an *AG* knockdown, we consistently observed the initiation of a large number of trichomes (16.7±1.8) on gynoecia (Table 1). Instead of the more scattered distribution typically found on *try* and *cpc* single-mutant gynoecia (Fig. 2F,G), these trichomes often clustered together (Fig. 2H-J), thus mimicking the characteristic pattern of trichome initiation on the leaves of *try cpc* double mutants (Schellmann et al., 2002). In these plants lacking AG, TRY and CPC activity, trichomes also consistently initiated at the distal tip of gynoecia and, remarkably, on the adaxial side of carpel valves, with trichomes forming adjacent to ovules (Fig. 2H-J). The latter phenotype was fully penetrant. Furthermore, a small number of trichomes (between one and four) formed at the distal tip and on the abaxial surface but never on the adaxial side of most (~80%) anthers (Fig. S4E). To confirm these observations, we generated and analyzed *ag-10 try cpc* triple mutants. Trichome initiation patterns in flowers of these plants were similar overall to those of ethanol-

Development (2018) 145, dev157784. doi:10.1242/dev.157784

treated AG-amiRNA^{AlcR} *try cpc* plants, with consistent trichome initiation on the outside of carpel valves (Fig. S4F) and on the abaxial side or distal tip of anthers (1.3±0.2) (Table 1). However, in these triple-mutant plants, we never observed trichome formation inside of the gynoecium, possibly as a consequence of the weak perturbation of C function in *ag-10* and different requirements for AG activity on the adaxial and abaxial sides of carpel valves (see Discussion). Taken together, these results show that *TRY*/*CPC* and the C and B function regulators all contribute to the suppression of trichome initiation on reproductive floral organs.

SPL transcription factors suppress trichome initiation on gynoecia

Given that we found several trichome repressor genes among genes associated with AG binding in a genome-wide localization study (Ó'Maoiléidigh et al., 2013), we considered the possibility that the C function protein is involved in the regulation of these genes during early floral stages. However, a comparison of two transcriptomics datasets (Ó'Maoiléidigh et al., 2015) showed that only two of the trichome repressors, *CPC* and *TRICHOMELESS1* (*TCL1*), were differentially expressed after AG perturbation in whole inflorescences (Fig. 2D; Table S2). To determine the effect of AG perturbation specifically in the fourth whorl, we collected gynoecia from stage ~9-13 flowers 24 h after an induced knockdown of AG for qRT-PCR analysis. In these assays, we detected perturbation of two other trichome repressors, whereas *TCL1* and *CPC* were not downregulated, compared with mock-treated control plants (Fig. S3E). Taken together with the continuous elevation in expression of most trichome repressors as flower development proceeds (Fig. 2A-C), these results do not support the conjecture that AG has a widespread role in promoting and maintaining the expression of trichome repressor genes during flower development.

SPL transcription factors have been shown to control trichome distribution on leaves, stems and sepals by directly promoting the expression of trichome repressor genes, including *TRY* and *TCL1* (Yu et al., 2010). Given that our genome-wide localization data for AG (Ó'Maoiléidigh et al., 2013) showed that four SPL genes are associated with AG binding (Fig. S5A-D), we hypothesized that AG promotes the expression of these genes in the reproductive floral organs, which in turn might lead to the observed upregulation of trichome repressor genes during early flower development. However, neither these nor other SPL genes were consistently differentially expressed after *AG* perturbation (Fig. S5E), suggesting that their expression does not depend on AG activity. Therefore, we tested whether the SPL genes act independently of *AG* in reproductive floral organs. To this end, we exploited the fact that the activity of several SPL genes is regulated in an age-dependent manner by members of the miR156 family of microRNAs (Rhoades et al., 2002; Wu et al., 2009). We combined the AG-amiRNA^{AlcR} transgenic line with a transgene that facilitates *MIR156B* overexpression (denoted miR156^{OE}) and leads to a reduction in *SPL* activity but not to the formation of trichomes on carpel valves (Fig. 3A) (Schwab et al., 2005; Yu et al., 2010) and found that an *AG* knockdown in this line led to significantly (P<0.001) more trichomes on gynoecia (21.2±0.6) than in AG-amiRNA^{AlcR} plants (8.0±0.3) (Fig. 3C; Table 1). Likewise, *ag-10* miR156^{OE} plants consistently formed trichomes on carpel valves (Fig. 3B), unlike either of the parental lines, in which gynoecia are completely glabrous (see above).

In further support of the hypothesis that the *SPL*/*miR156* pathway contributes to the suppression of trichome formation on gynoecia, we found that *AG* perturbation in plants mutant for two SPL genes, *SPL9* and *SPL15*, resulted in a significantly (P<0.001) increased number of trichomes on gynoecia (18.1±0.6 versus 8.0±0.3 in AG-amiRNA^{AlcR}; Table 1; gynoecia of mock-treated AG-amiRNA^{AlcR} *spl9 spl15* plants were completely glabrous) (Fig. 3D). This phenotype was slightly weaker than in the AG-amiRNA^{AlcR} miR156^{OE} line, suggesting that miR156 targets other than *SPL9* and *SPL15* also contribute to this process. Also, an *AG* knockdown in a background in which *miR156* activity is depleted through overexpression of a miRNA mimicry construct (Franco-Zorrilla et al., 2007) (denoted MIM156^{OE}) led to significantly (P<0.001) fewer trichomes on carpel valves compared with AG-amiRNA^{AlcR} alone (2.4±0.2 versus 8.0±0.3 in AG-amiRNA^{AlcR}) (Fig. 3E; Table 1). Lastly, we confirmed the direct involvement of SPL transcription factors in the suppression of trichome formation on carpel valves by analyzing the effects of an *AG* knockdown in an SPL9pro:GFP-rSPL9 background, in which a *miR156*-resistant version of *SPL9* is expressed from the *SPL9* promoter (Wang et al., 2009). The carpel valves of these plants were consistently completely glabrous, although other *ag*-like phenotypes were observed, confirming that an *AG* knockdown had occurred (Fig. 3F; Table 1). Together, these results demonstrate that the *SPL*/*miR156* pathway is active in reproductive floral organs and likely suppresses trichome formation independently of AG, in all probability by upregulating trichome repressor genes (Yu et al., 2010).

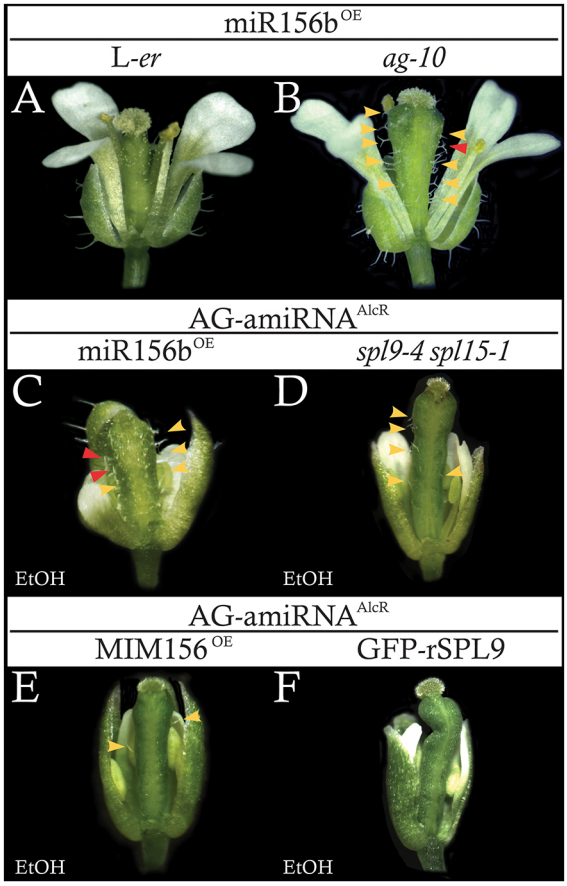

Fig. 3. Interaction between *AG* and the *SPL*/*miR156* pathway. (A-F) Genetic interactions between *AG* and *SPL*/*miR156*. (A,B) Flowers from (A) miR156^{OE} and (B) *ag-10* miR156^{OE} plants. (C-F) Flowers from ethanol (EtOH)-treated (C) AG-amiRNA^{AlcR} miR156^{OE}, (D) AG-amiRNA^{AlcR} *spl9 spl15*, (E) AG-amiRNA^{AlcR} MIM156^{OE} and (F) AG-amiRNA^{AlcR} SPL9pro:GFP-rSPL9 plants. Yellow and red arrowheads indicate simple or two-branched trichomes and three-branched trichomes, respectively. See Table 1 for details.

Development (2018) 145, dev157784. doi:10.1242/dev.157784

AG controls cytokinin responsiveness in the gynoecium

Phytohormones are known to promote trichome initiation on leaves, with the activities of gibberellins, jasmonic acid and cytokinin being conserved between certain clades of flowering plants (Maes and Goossens, 2010). Given that we had identified several genes related to hormone responses as putative direct AG targets (Table S3; O'Maoileidigh et al., 2013), we sought to understand whether AG modulates responses to these hormones to suppress trichome formation on floral organs. To test this, we treated AG-amiRNA^{AlcR} plants with solutions containing 100 µM of gibberellic acid (GA_3), methyl jasmonate (MeJA), or cytokinin 6-benzylaminopurine (BAP), or with a mock solution, and determined the number of trichomes that formed on gynoecia in the presence and absence of AG activity. Although none of the treatment regimens induced trichome initiation on carpel valves when AG was active (Table 1), all hormone treatments (but not the mock treatment) led to a significant (P<0.001) increase in trichome numbers after AG perturbation. This increase was particularly strong in the presence of BAP (Fig. 4A,B), and was found to be linearly correlated with the BAP concentration used (Table 1). In agreement with the idea that cytokinins have a major role in the control of trichome initiation on gynoecia, trichomes (23.7±1.1) formed consistently on carpel valves of BAP-treated *ag-10* plants (Fig. 4C; Table 1), whereas GA_3 and MeJA-treated (as well as mock-treated) *ag-10* gynoecia remained completely glabrous (Table 1), likely as a consequence of the weak perturbation of C function in *ag-10*. Taken together, these results suggest that AG suppresses trichome formation in part by limiting the cytokinin response in the gynoecium.

Given that we had found three type-A *ARABIDOPSIS RESPONSE REGULATORS* (ARRs), which negatively regulate cytokinin responses and are induced transcriptionally by the application of exogenous cytokinins (Hwang et al., 2012), among putative direct targets of AG (Ó'Maoiléidigh et al., 2013) (Fig. 4D-F; Table S3), we considered the possibility that the observed cytokinin hypersensitivity after *AG* perturbation was caused by misregulation

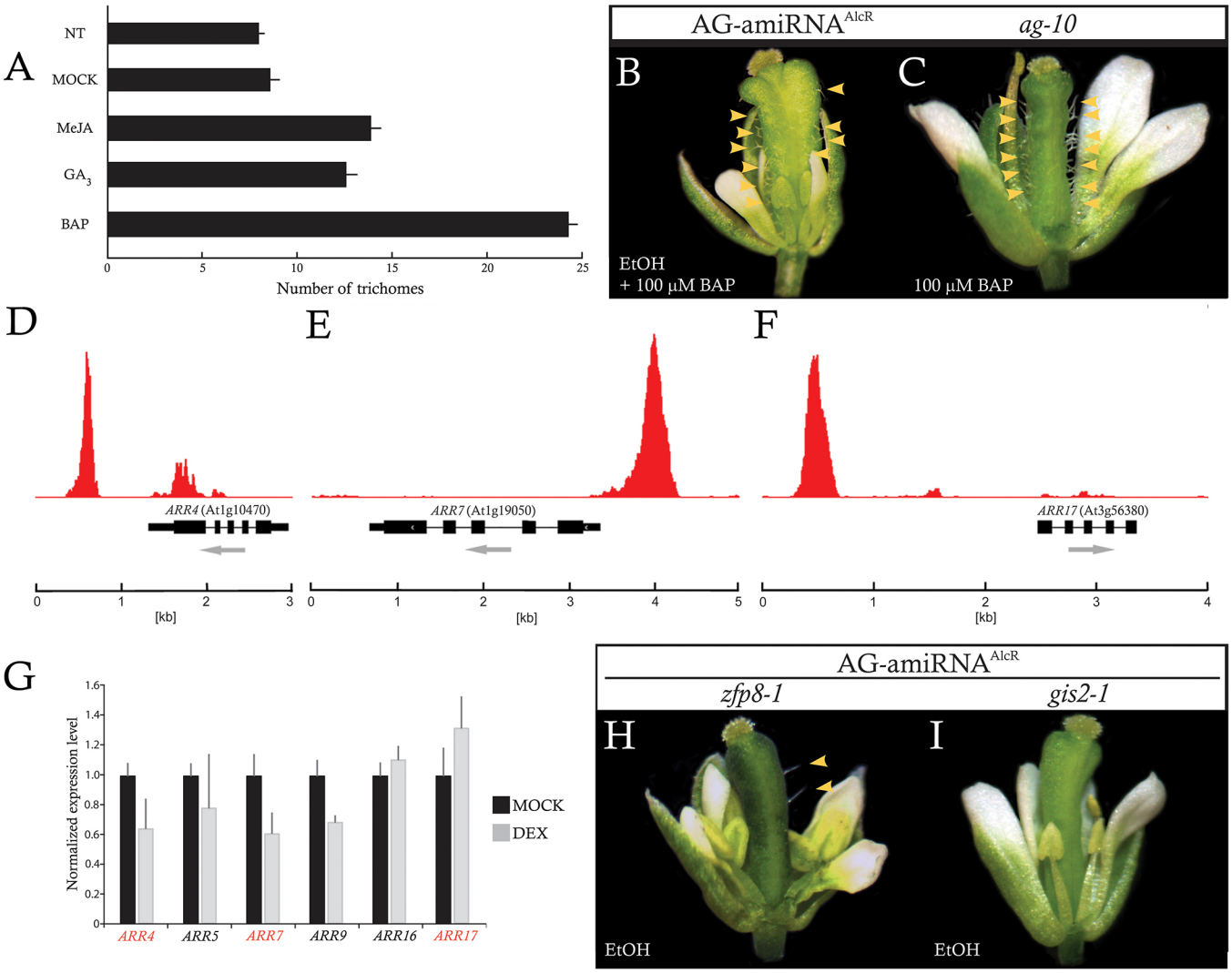

Fig. 4. Interplay between cytokinin and AG during gynoecium development. (A) Trichome numbers on gynoecia of AG-amiRNA^{AlcR} plants after *AG* knockdown and treatment with 100 µM MeJA, GA_3, BAP, a mock solution, or without an additional treatment (NT). Error bars represent s.e.m. See Table 1 and Table S1 for details. (B,C) Flowers from (B) ethanol-treated AG-amiRNA^{AlcR} and (C) *ag-10* plants after treatment with BAP. (D-F) ChIP-Seq results showing AG binding near ARR genes. The exon-intron structure and the direction of transcription (arrow) for each gene are indicated. Data are from O'Maoileidigh et al. (2013). (G) Expression of selected cytokinin response genes in gynoecia of AG-amiRNA$^{GR\text{-}LhG4}$ plants after *AG* knockdown. Data were normalized to mock-treated samples. Genes highlighted in red were associated with AG binding. Data represent the mean of three biological replicates, error bars represent s.e.m. (H,I) Flowers from ethanol-treated (H) AG-amiRNA^{AlcR} *zfp8* and (I) AG-amiRNA^{AlcR} *gis2* plants. Arrowheads indicate simple or two-branched trichomes. See Table 1 for details.

Development (2018) 145, dev157784. doi:10.1242/dev.157784

of these genes. To test the effect of AG on these ARRs, we monitored their response, as well as that of three other type-A ARRs that are not putative direct AG targets, to *AG* perturbation specifically in gynoecia. In this experiment, we observed a decrease in expression of three of the six ARRs tested, two of which are associated with AG binding (Fig. 4G). Thus, AG might limit cytokinin sensitivity in the gynoecium by promoting, directly or indirectly, the expression of several type-A ARR repressor proteins.

To understand better the interplay between AG and cytokinin in the suppression of trichome formation, we investigated the genetic interactions between AG and two C2H2 transcription factors, ZFP8 and GIS2, which promote trichome formation on cauline leaves, stems and sepals in a cytokinin-dependent manner (Gan et al., 2007). We had previously identified *ZFP8*, but not *GIS2*, as a possible indirect target gene of AG (Ó'Maoiléidigh et al., 2013). We found a significant (P<0.001) reduction in the number of trichomes that formed on gynoecia of *zfp8* and *gis2* mutant plants after AG perturbation, with the effect being considerably stronger in *gis2* (0.1±0.1) than in *zfp8* (1.5±0.2; 8.0±0.3 in AG-amiRNA^{AlcR}) (Fig. 4H,I; Table 1). Therefore, the ectopic formation of trichomes on AG-amiRNA^{AlcR} gynoecia is dependent on *GIS2* and, to a lesser extent, *ZFP8* activity.

Try/*cpc* mutants exhibit cytokinin hypersensitivity

Given that our results showed that gynoecia are hypersensitive to cytokinin treatment after a knockdown of AG, and that AG and TRY/CPC act in a partially redundant manner in the suppression of trichome formation, we tested whether *try*/*cpc* mutants also exhibit cytokinin hypersensitivity. To this end, we treated inflorescences of *try* and *cpc* single mutants and of *try cpc* double-mutant plants with BAP. Whereas the reproductive organs of BAP-treated *cpc* plants remained completely glabrous (Table 1), approximately 30% of equally treated *try* mutant flowers formed trichomes on carpel valves, stigma and anthers (Fig. S6A-C). By contrast, the reproductive floral organs of *try cpc* double mutants consistently carried trichomes after BAP treatment (Fig. S6D) and were phenotypically similar to *try cpc* plants, with reduced AG activity (Fig. 2H,I; Fig. S4D-F) although we never observed trichomes on the adaxial side of carpel valves. We next tested the effect of a perturbation of AG activity in tandem with BAP treatment in these genetic backgrounds. Whereas in *cpc* or *try* single mutants, trichome numbers on gynoecia were not or only slightly increased compared with a wild-type background (22.2±1.1 in *cpc*; 27.0±2.2 in *try*; 24.3±0.7 in the wild type), *try cpc* double mutants displayed a strongly enhanced trichome initiation pattern (>35 trichomes on average per gynoecium) on reproductive floral organs (Fig. 5). Taken together, the results of these experiments show that a perturbation of *TRY*, *CPC* and *AG* leads to increased cytokinin hypersensitivity in carpel valves relative to *AG* knockdown alone.

KAN1 and AG act together in the control of trichome initiation and organ polarity

While conducting BAP treatments, we noted in approximately 30% of flowers the formation of outgrowths from the replum in the medial

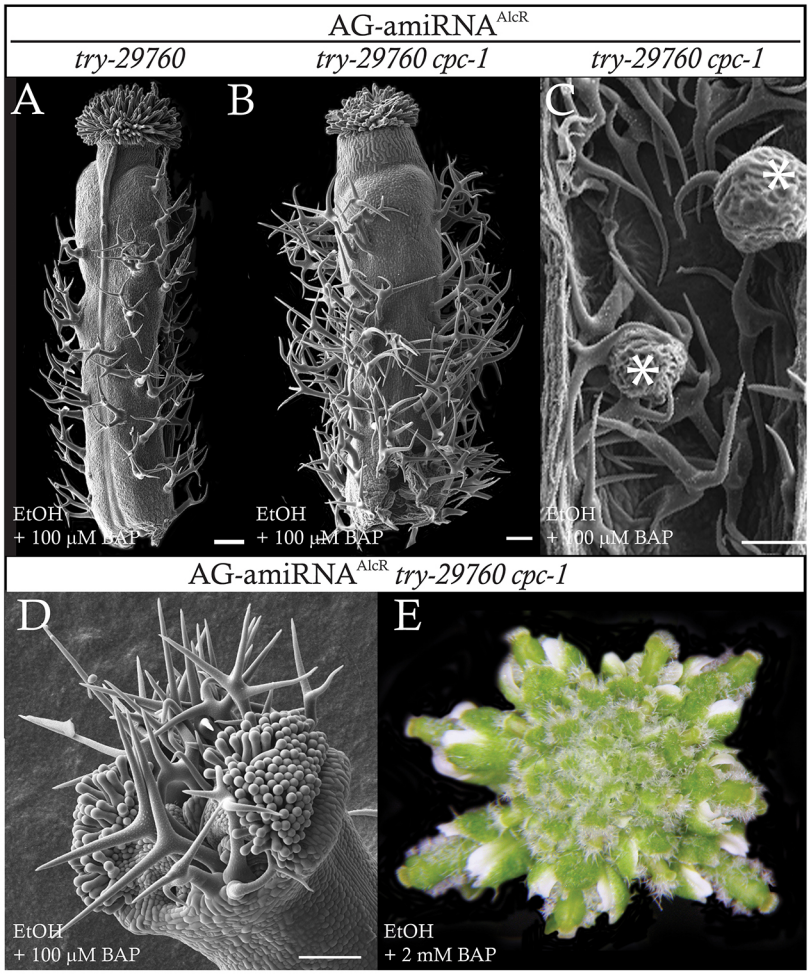

Fig. 5. Cytokinin hypersensitivity in flowers of plants lacking *AG*, *TRY* and *CPC* activity. (A-D) Scanning electron micrographs of gynoecia from plants simultaneously treated with ethanol (EtOH) vapor and 100 µM BAP. (A) An AG-amiRNA^{AlcR} *try* gynoecium. (B) An AG-amiRNA^{AlcR} *cpc try* gynoecium. (C) The adaxial surface of a dissected AG-amiRNA^{AlcR} *cpc try* gynoecium. Asterisks indicate ovules. (D) The stigma of an AG-amiRNA^{AlcR} *try cpc* gynoecium. (E) The inflorescence of an AG-amiRNA^{AlcR} *cpc try* plant after treatment with ethanol vapor and 2 mM BAP. A higher BAP concentration was used in this experiment to assess the phenotypic range. Scale bars: 200 µm (A,B); 100 µm (C,D). See Table 1 for details.

Development (2018) 145, dev157784. doi:10.1242/dev.157784

region of *try* but not of *cpc* or *try cpc* gynoecia (Fig. S7A,B,D-F). When *AG* was perturbed in BAP-treated *try* mutants, this phenotype increased in strength and small gynoecium-like structures formed close to the replum (Fig. S7C). This phenotype was especially apparent in flowers that were at early stages of development at the time of BAP treatment, whereas flowers that were at more advanced stages of development were more likely to initiate trichomes (Fig. 5A). A similar phenotype had been previously reported when wild-type plants were repeatedly sprayed with a solution containing 100 µM BAP (Marsch-Martínez et al., 2012). However, under our conditions, where we applied an equally concentrated BAP solution specifically to inflorescences only once, wild-type plants never exhibited such outgrowths. Thus, it appears that the above-mentioned cytokinin hypersensitivity in gynoecia of plants with reduced AG and TRY activity not only affects trichome initiation, but also leads to abnormal development of the medial domain.

Notably, BAP-treated *try* gynoecia are reminiscent of gynoecia of *kan1* mutants. *KAN1* was originally identified in a genetic screen for plants that prematurely produce abaxial trichomes on rosette leaves (Kerstetter et al., 2001). Subsequently, it was demonstrated that the KAN1 transcription factor redundantly specifies abaxial identity of lateral organs (Kerstetter et al., 2001), including gynoecia, where it is also involved in establishing apical-basal polarity (Pires et al., 2014). Thus, KAN1 controls trichome formation in leaves, cell proliferation in the medial region of the gynoecium and, more generally, organ polarity. To determine whether these functions depend on cytokinin signaling, we tested the response of a weak *kan1* mutant allele to BAP treatment. In agreement with a hypersensitive response to cytokinin, the outgrowths from *kan1* gynoecia were more pronounced compared with untreated samples (Fig. 6A,B). Also, trichomes initiated sporadically on the abaxial side of carpel valves (Fig. 6C). Given that both *kan1* and *ag* mutants are hypersensitive to exogenous cytokinin treatments, and in a comparison of datasets from genome-wide localization studies for KAN1 (Merelo et al., 2013) and AG (Ó'Maoiléidigh et al., 2013), we found that they share many putative direct targets (Fig. S8A; Table S4), we generated AG-amiRNA^{AlcR} *kan1* plants to test whether AG and KAN1 act together in the control of gynoecium development. After *AG* perturbation, these plants bore significantly (P<0.001) more trichomes on gynoecial valves than in corresponding plants with a functional *KAN1* allele (26.6±0.8 versus 8.0±0.3 in AG-amiRNA^{AlcR}), whereas medial outgrowths were more severe compared with *kan1* single mutants (Fig. 6D). Finally, we perturbed AG activity in *kan1* mutants while simultaneously treating plants with BAP and found that these treatments induced ovule development apically on the outer side of the gynoecium, while simultaneously increasing trichome numbers (to 32.2±0.8) (Fig. 6E,F). Thus, AG and KAN1 appear to act together in the (cytokinin-dependent) control of trichome initiation, development of the medial region, and abaxial-adaxial polarity of the gynoecium.

DISCUSSION

The activation of regulatory modules that control trichome distribution in plants occurs at different stages of post-embryonic development: in the first true leaves that are formed, regulators of

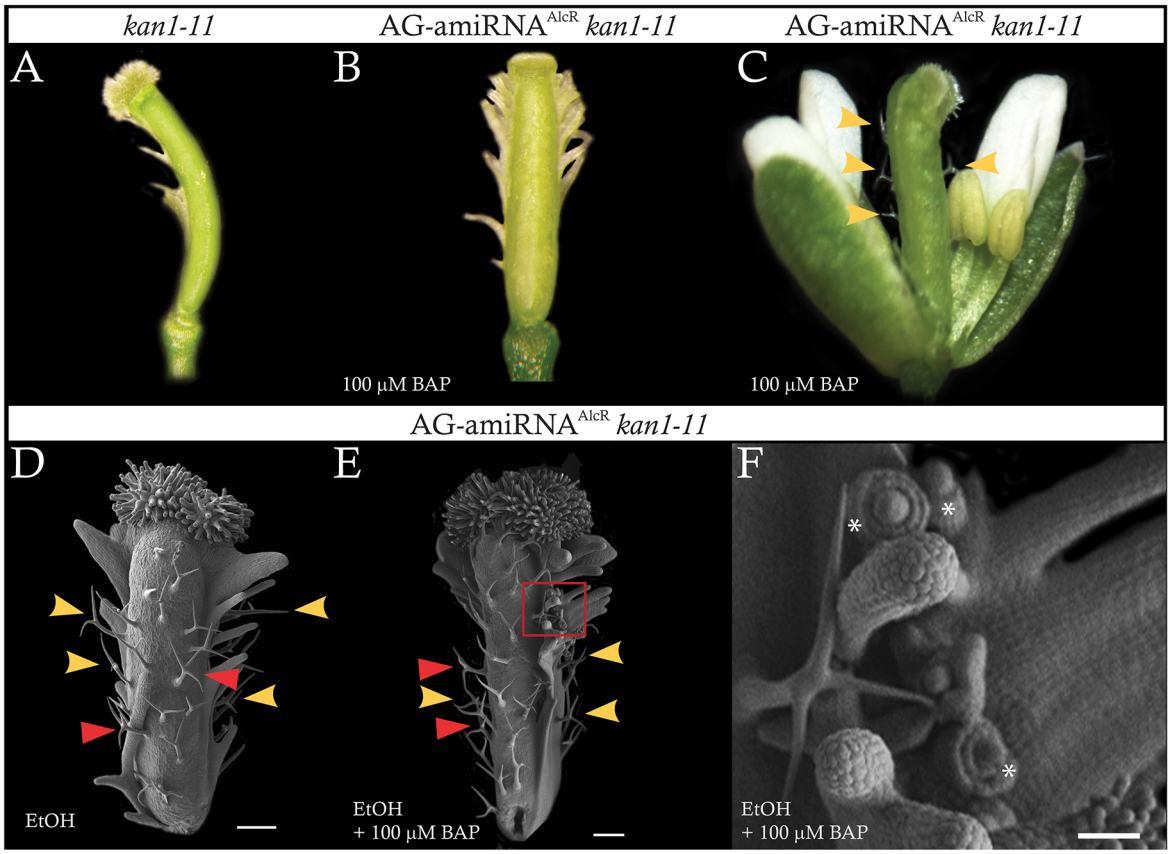

Fig. 6. Interactions between KAN1 and AG during gynoecium development. (A) A gynoecium from a *kan1* plant. (B,C) A gynoecium and a flower from a *kan1* plant after 100 µM BAP treatment. (D-F) Scanning electron micrographs of AG-amiRNA^{AlcR} *kan1* plants after (D) ethanol (EtOH) vapor treatment or (E,F) simultaneous ethanol vapor and 100 µM BAP treatments. (F) Enlargement of the boxed region in E. Yellow and red arrowheads indicate simple or two-branched trichomes and three-branched trichomes, respectively. Asterisks mark ovule primordia. Scale bars: 200 µm (D,E); 25 µm (F). See Table 1 for details.

Development (2018) 145, dev157784. doi:10.1242/dev.157784

organ polarity, such as KAN1, likely ensure that trichomes are initiated exclusively adaxially (Chien and Sussex, 1996; Kerstetter et al., 2001; Telfer et al., 1997). As development continues, the age-dependent activation of the *SPL*/*miR156* pathway leads to a gradual redistribution of trichomes from the adaxial to the abaxial side (Wu et al., 2009). This redistribution process appears to depend largely on the upregulation of trichome repressor genes (Yu et al., 2010) and reaches completion in early-arising sepals that carry trichomes only abaxially. Petals, stamens and carpels, which are initiated following the emergence of sepal primordia (Smyth et al., 1990), are typically devoid of trichomes. Both the present as well as a previous (Ó'Maoiléidigh et al., 2013) study demonstrated that floral homeotic proteins, including B and C function regulators and SHP1/2, are required for the complete suppression of trichome formation on reproductive floral organs (and possibly also on petals, which we did not test here). Furthermore, we found that key components of the trichome distribution network, such as *KAN1* and the *SPL*/*miR156* pathway, are involved in the suppression of trichome initiation during gynoecium development (Fig. 7). Thus, the control of trichome formation in these organs appears to be mediated by both flower-specific inputs and regulatory pathways that are an integral part of the genetic program for leaf development and that remain active during floral organ morphogenesis.

The combined results of our genetic, genomic and molecular analyses suggest that the activities of the floral homeotic proteins are superimposed onto the trichome distribution network: AG appears to suppress trichome initiation in part by targeting key trichome regulators, such as *GL1* and certain trichome repressor genes. However, a perturbation of AG activity had only relatively weak effects on the expression of these genes, implying that additional pathways might contribute to this process. In fact, our results suggest that the AG-dependent control of cytokinin signaling is crucial for the suppression of floral trichome formation. We found that AG promotes, in some cases directly, the expression of negative regulators of cytokinin signaling in gynoecia and that the trichome phenotype we observed after AG perturbation depends on ZFP8 and GIS2, which promote trichome formation in a cytokinin-dependent manner. Given that cytokinin has important roles during the formation and patterning of the gynoecium (Marsch-Martínez et al., 2012) and that AG is broadly expressed in the female reproductive organ, the observed effect on cytokinin signaling is unlikely to be limited to the control of trichome initiation. In fact, our data imply that AG is also involved in the cytokinin-dependent control of cell proliferation in the medial domain and, together with KAN1, regulates abaxial-adaxial polarity in the gynoecium. The latter role is in agreement with our results from genome-wide surveys (Ó'Maoiléidigh et al., 2013), which revealed several regulators of organ polarity, such as *CRC* and *KAN2*, as likely direct targets of AG (Table S2; Fig. 2D; Fig. S8B).

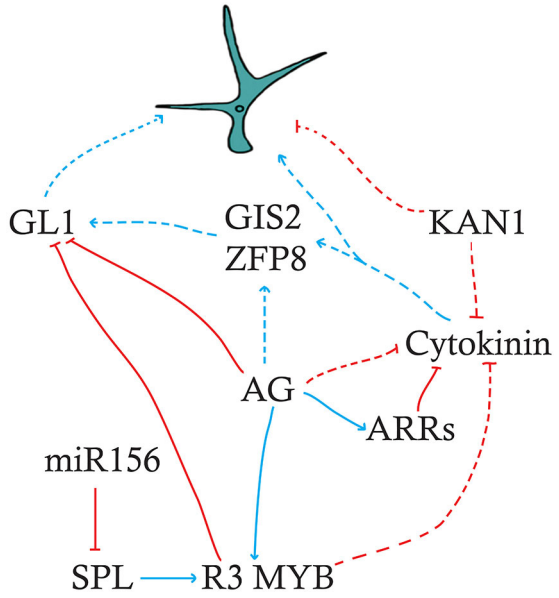

Fig. 7. A model for the suppression of trichome initiation on gynoecia. Blue lines with arrowheads indicate positive regulation, whereas red capped lines indicate negative regulation. Solid lines indicate direct regulation and dashed lines either indirect regulation or an unknown mechanism. AG directly controls the expression of trichome regulators (e.g. *GL1*, *CPC*), while also controlling cytokinin responses through direct regulation of type-A ARRs, and indirect regulation of cytokinin response genes, such as *ZFP8* (O'Maoileidigh et al., 2013). The *SPL* and *KAN1* transcription factors suppress trichome formation in parallel with AG through partially overlapping mechanisms.

The introduction of a revised ABCE model with more widespread applicability for diverse angiosperms led to the proposal that sepals represent the ground state of a floral organ, which is then altered by B, C and E function proteins to give rise to petals, stamens and carpels (Causier et al., 2010). Thus, the internal floral organs could be, strictly speaking, not modified leaves but modified sepals. In agreement with this idea, the results of our genetic analyses showed that the floral homeotic proteins are mainly needed to suppress the formation of abaxial trichomes, which is a characteristic feature of sepals. However, at least AG appears to also be involved in controlling trichome initiation on the adaxial side of gynoecial valves, possibly as an indirect consequence of its other functions during gynoecium development (Pinyopich et al., 2003) and its resulting broad expression domain (Ito et al., 2004; Yanofsky et al., 1990). In contrast to the abaxial side, the role of AG in suppressing adaxial trichomes on carpel valves is masked by the activities of *TRY* and *CPC* (and possibly other trichome repressor genes), which likely act at least in part downstream of the *SPL*/*miR156* pathway (Yu et al., 2010).

As described in the Introduction, many angiosperm species form abaxial and even adaxial trichomes on gynoecia to protect developing fruits and seed pods from herbivory. Whereas the molecular basis of these phenotypes is currently unknown, from our data it can be hypothesized that a modification of C function (relative to that observed in *Arabidopsis*) led to the formation of these gynoecial trichomes. For example, the disruption or the creation of one or more AG-binding sites in the promoter of a trichome regulatory gene or a gene involved in cytokinin signaling might be sufficient to overcome the inhibitory effect of AG on trichome initiation, at least on the abaxial side of carpel valves. Such minor genetic changes could also explain the great diversity in trichome initiation patterns in flowers observed among members of a single family, such as the Brassicaceae. With recent advances in genome sequencing and the relative ease with which new models for plant research can now be established, testing this hypothesis should be feasible in the near future.

MATERIALS AND METHODS

Plant materials and growth

Plants for genetic experimentation were grown on a soil:vermiculite:perlite (3:1:1) mixture at 20°C under constant illumination with cool white fluorescent light, except for miR156^{OE} and *ag-10* miR156^{OE} plants in a Landsberg *erecta* (L-*er*) background and plants for qRT-PCR analysis, which were grown in 16 h-long daylight conditions at 21°C. Plant lines used in this study are listed in Table S5.

Development (2018) 145, dev157784. doi:10.1242/dev.157784

Genotyping

Genotyping PCRs were performed with genomic DNA extracted as described by Edwards et al. (1991). PCRs for cloning purposes were performed using DNA extracted as described by Clarke (2009). Primers are listed in Table S6.

Cloning of OPpro:SHP2-GFP

cDNA derived from RNA extracts of flowers was amplified with primers DM722 and DM723 (Table S6). This amplicon was incubated with *Sal*I and *Mlu*I and ligated to pBJ36-GFP, which was cut with the same enzymes to generate pBJ36-SHP2-GFP. The SHP2-GFP fragment was subcloned downstream of the 6xOP promoter in pBJ36-6xOP using *Xho*I and *Bam*HI. To generate the binary vector, the 6xOP-SHP2-GFP fragment was subcloned to pML-BART-35Spro:GR-LhG4 using *Not*I. This vector was transformed into *Agrobacterium* strain C58 pGV2260 (McBride and Summerfelt, 1990).

Expression of miR156 in L-*er* and *ag-10*

Both wild-type (accession: L-*er*) and *ag-10* plants were transformed with *Agrobacterium* strain pGV3101 harboring a binary vector containing the 35Spro:miR156b transgene (Wang et al., 2009). Transformants were selected with BASTA (Bayer). Seven L-*er* plants containing the 35Spro:miR156b transgene were identified, and these presented with miR156 overexpression phenotypes that have been previously described (Wang et al., 2009). Thirty-two *ag-10* plants containing the 35Spro:miR156b transgene were identified, all of which exhibited pubescent carpel valves along with other previously described miR156 overexpression phenotypes (Wang et al., 2009).

Plant transformation and selection

Agrobacterium-mediated plant transformation was carried out using the floral-dip method. A vacuum of 500 mbar was applied for 5 min while the inflorescences were submerged in the transformation solution. First-generation transgenic seedlings were identified by spraying seedlings with 200 µg/ml ammonium-glufosinate.

Ethanol vapor treatments

Treatments were performed for 24 h as previously described (Ó'Maoiléidigh et al., 2013).

Hormone treatments

Inflorescences were treated once with a few drops of a solution containing 100 µM 6-benzylaminopurine (Sigma), unless otherwise stated, methyl jasmonate (Sigma) or GA_3 (Duchefa Biochemie) and 0.015% (v/v) Silwett-77 (De Sangosse) using a Pasteur pipette. BAP stocks were prepared in distilled water with gibberellic acid and jasmonic acid prepared in ethanol. Mock treatments were identical except for the absence of the hormone.

Dexamethasone treatments

Plants were treated with a solution containing 10 µM dexamethasone, 0.015% (v/v) Silwet L-77 and 0.1% ethanol either using a Pasteur pipette to wet the inflorescence (for genetic analysis) or by dipping the inflorescences in the solution (for expression analysis). Mock treatments were identical except for the omission of dexamethasone.

Trichome counts

Carpel valves were monitored at anthesis for the presence of trichomes from several days after treatment until trichomes no longer formed on successive flowers. The full activation of the AG-amiRNA was determined by the presence of other *ag*-like phenotypes, such as bent gynoecia, shortened stamens and floral meristem indeterminacy.

Scanning electron microscopy

Floral organs were dissected from the main inflorescence and mounted on a glue and graphene mixture 1:1 (v:v). The tissue was immersed into liquid nitrogen for up to 1 min in a vacuum and transferred to an airtight scanning electron microscopy (SEM) cryochamber (−140°C). The sample was sublimed for 30 s to −80°C to remove excess surface water. The sample was chilled to −140°C and sputtered with gold for imaging. All images were acquired using a Zeiss Ultra Plus SEM. Assistance was provided by the Centre for Microscopy and Analysis (Trinity College Dublin, Ireland).

Image processing

Images were processed with Adobe Photoshop to darken the background and to normalize the color to make the images clearer. Backgrounds of several scanning electron micrographs were removed in the same way. These modifications do not alter the interpretation of the data, and all original unmodified images are available on request.

Tissue harvesting

After plants had flowered, inflorescences were treated with either a mock or dexamethasone-containing solution. Carpels were harvested after 24 h from flowers of approximately stage 9-13 (Smyth et al., 1990) from exactly 15 individual plants.

RNA extraction and processing

RNA was extracted with a Qiagen RNeasy mini kit. RNA was quantified using a Thermo Fisher Nanodrop. Ten micrograms of RNA was used in a DNaseI digestion according to the manufacturer's instructions (Ambion Turbo DNA-free kit).

Statistical analysis

Statistical tests to compare trichome numbers between plant lines were performed with SigmaStat 3.5. The statistical significance of the overlap between putative direct targets of AG and KAN1 was determined with a hypergeometric distribution method (http://nemates.org/MA/progs/overlap_stats.html).

cDNA synthesis and quantitative real-time PCR

One microgram of DNA-free RNA was heated to 65°C before adding SuperScript II reverse transcriptase (Invitrogen), RNaseOUT (Invitrogen), First Strand buffer (Invitrogen), Oligo$(dT)_{18}$ (Sigma), and dNTPs (Thermo Fisher) according to the manufacturers' instructions. The reaction was incubated at 42°C for 50 min and then at 70°C for 10 min. qRT-PCR was performed using 1 µl of a dilution of the cDNA synthesis reaction in a 10 µl reaction. The iQ™ SYBR Green Supermix (Bio-Rad) was used according to the manufacturer's instructions. The reaction was run on a LightCycler 480 (Roche) and measurements were taken for three biological replicates; all PCRs were performed twice (technical duplicates). Melting curve analysis was also performed, revealing a single peak for each PCR reaction. The amplification data were analyzed using the second derivative maximum method, and resulting Cp values were converted into relative expression values using the comparative cycle threshold method. The *PP2AA3* (*At1g13320*) gene was used to normalize the data (Czechowski et al., 2005).

Acknowledgments

We thank Ailbhe Brazel, Serena Della Pinna, Youbong Hyun and Maida Romera-Branchat for critical comments on the manuscript.

Competing interests

The authors declare no competing or financial interests.

Author contributions

Conceptualization: D.S.Ó'M., F.W.; Methodology: D.S.Ó'M., D.S., F.W.; Validation: D.S.Ó'M., F.W.; Formal analysis: D.S.Ó'M., B.Z.; Investigation: D.S.Ó'M., D.S., F.W.; Resources: G.C., F.W.; Data curation: D.S.Ó'M., F.W.; Writing - original draft: D.S.Ó'M., D.S., F.W.; Writing - review & editing: D.S.Ó'M., D.S., B.Z., G.C., F.W.; Visualization: D.S.Ó'M., D.S., B.Z., F.W.; Supervision: D.S.Ó'M., F.W.; Project administration: D.S.Ó'M., F.W.; Funding acquisition: D.S.Ó'M., G.C., F.W.

Funding

This study was supported by grants from Science Foundation Ireland (10/IN.1/B2971 and 16/IA/4559 to F.W.) and the Environmental Protection Agency (16/IA/4559 to F.W.) under the Investigators Programme. D.S.Ó'M. was supported in part by an

Alexander von Humboldt-Stiftung Research Fellowship. B.Z. was supported in part by a postdoctoral fellowship from the Irish Research Council (GOIPD/2015/267).

Supplementary information

Supplementary information available online at
http://dev.biologists.org/lookup/doi/10.1242/dev.157784.supplemental

References

Bowman, J. L., Smyth, D. R. and Meyerowitz, E. M. (1989). Genes directing flower development in Arabidopsis. *Plant Cell* **1**, 37-52.

Bowman, J. L., Drews, G. N. and Meyerowitz, E. M. (1991). Expression of the Arabidopsis floral homeotic gene AGAMOUS is restricted to specific cell types late in flower development. *Plant Cell* **3**, 749-758.

Causier, B., Schwarz-Sommer, Z. and Davies, B. (2010). Floral organ identity: 20 years of ABCs. *Semin. Cell Dev. Biol.* **21**, 73-79.

Chien, J. C. and Sussex, I. M. (1996). Differential regulation of trichome formation on the adaxial and abaxial leaf surfaces by gibberellins and photoperiod in Arabidopsis thaliana (L.) Heynh. *Plant Physiol.* **111**, 1321-1328.

Clarke, J. D. (2009). Cetyltrimethyl ammonium bromide (CTAB) DNA miniprep for plant DNA isolation. *Cold Spring Harb. Protoc.* **2009**, pdb prot5177.

Coen, E. S. and Carpenter, R. (1993). The metamorphosis of flowers. *Plant Cell* **5**, 1175-1181.

Czarna, A., Gawrońska, B., Nowińska, R., Morozowska, M. and Kosiński, P. (2016). Morphological and molecular variation in selected species of Erysimum (Brassicaceae) from Central Europe and their taxonomic significance. *Flora-Morphology, Distribution, Functional Ecology of Plants* **222**, 68-85.

Czechowski, T., Stitt, M., Altmann, T., Udvardi, M. K. and Scheible, W. R. (2005). Genome-wide identification and testing of superior reference genes for transcript normalization in Arabidopsis. *Plant Physiol.* **139**, 5-17.

Ditta, G., Pinyopich, A., Robles, P., Pelaz, S. and Yanofsky, M. F. (2004). The SEP4 gene of Arabidopsis thaliana functions in floral organ and meristem identity. *Curr. Biol.* **14**, 1935-1940.

Edwards, K., Johnstone, C. and Thompson, C. (1991). A simple and rapid method for the preparation of plant genomic DNA for PCR analysis. *Nucleic Acids Res.* **19**, 1349.

Franco-Zorrilla, J. M., Valli, A., Todesco, M., Mateos, I., Puga, M. I., Rubio-Somoza, I., Leyva, A., Weigel, D., García, J. A. and Paz-Ares, J. (2007). Target mimicry provides a new mechanism for regulation of microRNA activity. *Nat. Genet.* **39**, 1033-1037.

Gan, Y., Liu, C., Yu, H. and Broun, P. (2007). Integration of cytokinin and gibberellin signalling by Arabidopsis transcription factors GIS, ZFP8 and GIS2 in the regulation of epidermal cell fate. *Development* **134**, 2073-2081.

Gomez-Mena, C., de Folter, S., Costa, M. M., Angenent, G. C. and Sablowski, R. (2005). Transcriptional program controlled by the floral homeotic gene AGAMOUS during early organogenesis. *Development* **132**, 429-438.

Honma, T. and Goto, K. (2001). Complexes of MADS-box proteins are sufficient to convert leaves into floral organs. *Nature* **409**, 525-529.

Hwang, I., Sheen, J. and Müller, B. (2012). Cytokinin signaling networks. *Annu. Rev. Plant Biol.* **63**, 353-380.

Immink, R. G. H., Tonaco, I. A. N., de Folter, S., Shchennikova, A., van Dijk, A. D. J., Busscher-Lange, J., Borst, J. W. and Angenent, G. C. (2009). SEPALLATA3: the 'glue' for MADS box transcription factor complex formation. *Genome Biol.* **10**, R24.

Ito, T., Wellmer, F., Yu, H., Das, P., Ito, N., Alves-Ferreira, M., Riechmann, J. L. and Meyerowitz, E. M. (2004). The homeotic protein AGAMOUS controls microsporogenesis by regulation of SPOROCYTELESS. *Nature* **430**, 356-360.

Ji, L., Liu, X., Yan, J., Wang, W., Yumul, R. E., Kim, Y. J., Dinh, T. T., Liu, J., Cui, X., Zheng, B. et al. (2011). ARGONAUTE10 and ARGONAUTE1 regulate the termination of floral stem cells through two microRNAs in Arabidopsis. *PLoS Genet.* **7**, e1001358.

Kerstetter, R. A., Bollman, K., Taylor, R. A., Bomblies, K. and Poethig, R. S. (2001). KANADI regulates organ polarity in Arabidopsis. *Nature* **411**, 706-709.

Krizek, B. A. and Fletcher, J. C. (2005). Molecular mechanisms of flower development: an armchair guide. *Nat. Rev. Genet.* **6**, 688-698.

Lamb, R. J. (1980). Hairs protect pods of mustard (brassica hirta 'gisilba') from flea beetle feeding damage. *Can. J. Plant Sci.* **60**, 1439-1440.

Liljegren, S. J., Ditta, G. S., Eshed, Y., Savidge, B., Bowman, J. L. and Yanofsky, M. F. (2000). SHATTERPROOF MADS-box genes control seed dispersal in Arabidopsis. *Nature* **404**, 766-770.

Maes, L. and Goossens, A. (2010). Hormone-mediated promotion of trichome initiation in plants is conserved but utilizes species- and trichome-specific regulatory mechanisms. *Plant Signal Behav.* **5**, 205-207.

Maes, L., Inze, D. and Goossens, A. (2008). Functional specialization of the TRANSPARENT TESTA GLABRA1 network allows differential hormonal control of laminal and marginal trichome initiation in Arabidopsis rosette leaves. *Plant Physiol.* **148**, 1453-1464.

Marsch-Martínez, N., Ramos-Cruz, D., Irepan Reyes-Olalde, J., Lozano-Sotomayor, P., Zuniga-Mayo, V. M. and de Folter, S. (2012). The role of cytokinin during Arabidopsis gynoecia and fruit morphogenesis and patterning. *Plant J.* **72**, 222-234.

McBride, K. E. and Summerfelt, K. R. (1990). Improved binary vectors for Agrobacterium-mediated plant transformation. *Plant Mol. Biol.* **14**, 269-276.

Merelo, P., Xie, Y., Brand, L., Ott, F., Weigel, D., Bowman, J. L., Heisler, M. G. and Wenkel, S. (2013). Genome-wide identification of KANADI1 target genes. *PLoS ONE* **8**, e77341.

Ó'Maoiléidigh, D. S., Wuest, S. E., Rae, L., Raganelli, A., Ryan, P. T., Kwasniewska, K., Das, P., Lohan, A. J., Loftus, B., Graciet, E. et al. (2013). Control of reproductive floral organ identity specification in Arabidopsis by the C function regulator AGAMOUS. *Plant Cell* **25**, 2482-2503.

Ó'Maoiléidigh, D. S., Graciet, E. and Wellmer, F. (2014). Gene networks controlling Arabidopsis thaliana flower development. *New Phytol.* **201**, 16-30.

Ó'Maoiléidigh, D. S., Thomson, B., Raganelli, A., Wuest, S. E., Ryan, P. T., Kwaśniewska, K., Carles, C. C., Graciet, E. and Wellmer, F. (2015). Gene network analysis of Arabidopsis thaliana flower development through dynamic gene perturbations. *Plant J.* **83**, 344-358.

Oppenheimer, D. G., Herman, P. L., Sivakumaran, S., Esch, J. and Marks, M. D. (1991). A myb gene required for leaf trichome differentiation in Arabidopsis is expressed in stipules. *Cell* **67**, 483-493.

Payne, C. T., Zhang, F. and Lloyd, A. M. (2000). GL3 encodes a bHLH protein that regulates trichome development in arabidopsis through interaction with GL1 and TTG1. *Genetics* **156**, 1349-1362.

Pelaz, S., Tapia-López, R., Alvarez-Buylla, E. R. and Yanofsky, M. F. (2001). Conversion of leaves into petals in Arabidopsis. *Curr. Biol.* **11**, 182-184.

Pinyopich, A., Ditta, G. S., Savidge, B., Liljegren, S. J., Baumann, E., Wisman, E. and Yanofsky, M. F. (2003). Assessing the redundancy of MADS-box genes during carpel and ovule development. *Nature* **424**, 85-88.

Pires, H. R., Monfared, M. M., Shemyakina, E. A. and Fletcher, J. C. (2014). ULTRAPETALA trxG genes interact with KANADI transcription factor genes to regulate arabidopsis gynoecium patterning. *Plant Cell* **26**, 4345-4361.

Rhoades, M. W., Reinhart, B. J., Lim, L. P., Burge, C. B., Bartel, B. and Bartel, D. P. (2002). Prediction of plant microRNA targets. *Cell* **110**, 513-520.

Ryan, P. T., Ó'Maoiléidigh, D. S., Drost, H.-G., Kwaśniewska, K., Gabel, A., Grosse, I., Graciet, E., Quint, M. and Wellmer, F. (2015). Patterns of gene expression during Arabidopsis flower development from the time of initiation to maturation. *BMC Genomics* **16**, 488.

Schellmann, S., Schnittger, A., Kirik, V., Wada, T., Okada, K., Beermann, A., Thumfahrt, J., Jürgens, G. and Hülskamp, M. (2002). TRIPTYCHON and CAPRICE mediate lateral inhibition during trichome and root hair patterning in Arabidopsis. *EMBO J.* **21**, 5036-5046.

Schwab, R., Palatnik, J. F., Riester, M., Schommer, C., Schmid, M. and Weigel, D. (2005). Specific effects of microRNAs on the plant transcriptome. *Dev. Cell* **8**, 517-527.

Shikata, M., Koyama, T., Mitsuda, N. and Ohme-Takagi, M. (2009). Arabidopsis SBP-box genes SPL10, SPL11 and SPL2 control morphological change in association with shoot maturation in the reproductive phase. *Plant Cell Physiol.* **50**, 2133-2145.

Smyth, D. R., Bowman, J. L. and Meyerowitz, E. M. (1990). Early flower development in Arabidopsis. *Plant Cell* **2**, 755-767.

Szymanski, D. B., Jilk, R. A., Pollock, S. M. and Marks, M. D. (1998). Control of GL2 expression in Arabidopsis leaves and trichomes. *Development* **125**, 1161-1171.

Telfer, A., Bollman, K. M. and Poethig, R. S. (1997). Phase change and the regulation of trichome distribution in Arabidopsis thaliana. *Development* **124**, 645-654.

Theissen, G. (2001). Development of floral organ identity: stories from the MADS house. *Curr. Opin. Plant Biol.* **4**, 75-85.

von Goethe, J. W. (1790). Versuch die Metamorphose der Pflanzen zu erklären. *Gotha, Germany: Ettinger*.

Walker, A. R., Davison, P. A., Bolognesi-Winfield, A. C., James, C. M., Srinivasan, N., Blundell, T. L., Esch, J. J., Marks, M. D. and Gray, J. C. (1999). The TRANSPARENT TESTA GLABRA1 locus, which regulates trichome differentiation and anthocyanin biosynthesis in Arabidopsis, encodes a WD40 repeat protein. *Plant Cell* **11**, 1337-1350.

Wang, S., Hubbard, L., Chang, Y., Guo, J., Schiefelbein, J. and Chen, J.-G. (2008). Comprehensive analysis of single-repeat R3 MYB proteins in epidermal cell patterning and their transcriptional regulation in Arabidopsis. *BMC Plant Biol.* **8**, 81.

Wang, J.-W., Czech, B. and Weigel, D. (2009). miR156-regulated SPL transcription factors define an endogenous flowering pathway in Arabidopsis thaliana. *Cell* **138**, 738-749.

Wu, G. and Poethig, R. S. (2006). Temporal regulation of shoot development in Arabidopsis thaliana by miR156 and its target SPL3. *Development* **133**, 3539-3547.

Wu, G., Park, M. Y., Conway, S. R., Wang, J.-W., Weigel, D. and Poethig, R. S. (2009). The sequential action of miR156 and miR172 regulates developmental timing in Arabidopsis. *Cell* **138**, 750-759.

Wuest, S. E., O'Maoileidigh, D. S., Rae, L., Kwasniewska, K., Raganelli, A., Hanczaryk, K., Lohan, A. J., Loftus, B., Graciet, E. and Wellmer, F. (2012). Molecular basis for the specification of floral organs by APETALA3 and PISTILLATA. *Proc. Natl. Acad. Sci. USA* **109**, 13452-13457.

Yanofsky, M. F., Ma, H., Bowman, J. L., Drews, G. N., Feldmann, K. A. and Meyerowitz, E. M. (1990). The protein encoded by the Arabidopsis homeotic gene agamous resembles transcription factors. *Nature* **346**, 35-39.

Development (2018) 145, dev157784. doi:10.1242/dev.157784

Yu, N., Cai, W.-J., Wang, S., Shan, C.-M., Wang, L.-J. and Chen, X.-Y. (2010). Temporal control of trichome distribution by microRNA156-targeted SPL genes in Arabidopsis thaliana. *Plant Cell* **22**, 2322-2335.

Zhao, M., Morohashi, K., Hatlestad, G., Grotewold, E. and Lloyd, A. (2008). The TTG1-bHLH-MYB complex controls trichome cell fate and patterning through direct targeting of regulatory loci. *Development* **135**, 1991-1999.